Published in final edited form as:

Transl Res. 2022 June ; 244: 101–113. doi:10.1016/j.trsl.2022.01.006.

In Vivo Cardiac-specific Expression of *Adenylyl Cyclase 4* Gene Protects against Klotho Deficiency-induced Heart Failure

Kai Chen[1,2], **Shirley Wang**[1,2], **Zhongjie Sun**[1,2]

[1]Department of Physiology, College of Medicine, University of Tennessee Health Science Center, Memphis, TN 38163, USA

[2]Department of Physiology, College of Medicine, University of Oklahoma Health Sciences Center, Oklahoma City, OK73104, USA

Abstract

Klotho is an aging-suppressor gene. *Klotho* gene deficiency causes heart failure in Klotho-hypomorphic mutant (KL (−/−)) mice. RNA-seq and western blot analysis showed that adenylyl cyclase type 4 (AC4) mRNA and protein expression was largely decreased in cardiomyocytes of KL (−/−) mice. The objective of this study was to investigate whether *in vivo* cardiac-specific expression of *AC4* gene protects against Klotho deficiency-induced heart failure. Interestingly, *in vivo* AAV-based cardiac-specific *AC4* gene expression increased left ventricular fractional shortening, ejection fraction, stroke volume, and left ventricular end-diastolic volume in KL (−/−) mice, suggesting that cardiac-specific *AC4* gene expression improves Klotho deficiency-induced heart dysfunction. Cardiac-specific *AC4* gene expression also decreased Klotho deficiency-induced cardiac hypertrophy. Cardiac-specific *AC4* gene expression alleviated Klotho deficiency-induced cardiac fibrosis and calcification. Furthermore, cardiac-specific *AC4* gene expression attenuated mitochondrial dysfunction, superoxide accumulation and cardiomyocyte apoptotic cell death. Thus, downregulation of AC4 may contribute to Klotho deficiency-induced heart failure. Mechanistically, AAV2/9-αMHC-AC4 increased cardiomyocytic cAMP levels and thus regulated the PKA-PLN-SERCA2 signal pathway, which is critical in modulating calcium flux and mitochondrial function. In conclusion, cardiac-specific *AC4* gene expression protects against Klotho deficiency-induced heart failure through increasing cardiomyocytic cAMP levels, which alleviates cAMP-dependent mitochondrial dysfunction, superoxide accumulation and apoptotic

Address Correspondence to: Dr. Zhongjie Sun, Professor and Chair, Department of Physiology, College of Medicine, University of Tennessee Health Science Center, A302 Coleman Building, 956 Court Avenue, Memphis, TN 38163, USA, Zsun10@uthsc.edu, Tel. 901-448-2679.

Author contributions: Conceptualization: ZS. Methodology: KC. Investigation: KC. Visualization: KC. Writing—original draft: KC. Writing—review & editing: ZS and KC. Funding acquisition: ZS

Conflict of Interest

None. All authors have read the journal's policy on disclosure of potential conflicts of interest.

Financial Disclosure

None.

Statement. All authors have read the journal's authorship agreement, and the manuscript has been reviewed by and approved by all named authors

cell death. AC4 regulates superoxide levels *via* the cAMP-PKA pathway. AC4 could be a potential therapeutic target for heart failure associated with Klotho deficiency.

Brief Commentary

Background.—Heart failure is the major cause of mortality in patients with chronic kidney disease (CKD). A decrease in Klotho levels is linked to CKD.

Translational significance.—We expect that treatment with Klotho or cardiac-specific expression of *AC4* gene would be effective in the control of heart failure in CKD patients. AAV is a safe vector and has been approved by FDA for clinical trial. AAV-αMHC-AC4 can be used for testing a novel cardiac-specific therapy for heart failure. Thus, the translation value of the finding is high.

Keywords

RNA-seq; Adenylyl cyclase; Klotho; heart failure; mitochondrial; apoptosis

Introduction

Heart disease caused 33% of deaths - almost one in every three-in the US [1]. Heart failure is the leading cause of death in the world. Despite substantial improvements in its management, including improved mechanical and pharmacological therapy, novel therapeutic approaches are required to improve outcomes for cardiovascular disease. Adenylyl cyclases (ACs) catalyze the conversion of ATP to adenosine 3', 5'-cyclic monophosphate (cAMP). cAMP is an important second messenger that regulates many aspects of cardiac physiology and pathology [2–4]. However, only recently have investigators explored the possibility that AC could serve as a therapeutic target for cardiomyopathy [5–10]. There are nine known isoforms of transmembrane adenylyl cyclases (tmACs) and one soluble adenylyl cyclase (sAC) in mammals [11]. Although AC5 and AC6 are the most abundant isoforms in the heart [5, 12], AC4 is also expressed in the heart. The function of AC4 in the heart is poorly understood. Whether AC4 plays a role in heart failure has never been investigated.

Klotho is an anti-ageing gene that was discovered in 1997 [13]. Mutation of the *klotho* gene in mice causes numerous symptoms of premature aging and shortens lifespan [13]. On the other hand, an increase in Klotho expression in mice yields extended lifespan [14], better cognitive function [15], resistance against induction of renal disease [16], cardiac disease [17], pulmonary disease [18], vascular calcification [19], diabetes [20, 21], while also acting as a tumor suppressor [22, 23]. Klotho levels declined in aging and chronic kidney disease (CKD) [24–27]. Klotho is related to numerous aging-related diseases. Recently, Klotho has gained much attention in cardiovascular disease which underscores its clinical significance [17, 28–30]. Our laboratory and other researchers found that Klotho deficiency causes heart failure and, further, that exogenous Klotho protects against aging- or chronic kidney disease-induced cardiomyopathy [17, 28, 31, 32]. Klotho hypomorphic mice have an insertional mutation in the 5′ upstream region of the *klotho* gene, resulting in undetectable *klotho* mRNA levels in organs that normally express the *klotho* gene [13]. The Klotho

hypomorphic mice show Klotho deficiency, which lead to premature aging phenotypes [24, 29]. The Klotho-deficient mouse is a powerful animal model for studying aging-related cardiovascular diseases.

In this study, we aimed to investigate the protective effects of AC4 on Klotho deficiency-induced cardiomyopathy. First, we constructed a rAAV2/9 vector in which the truncated αMHC promoter drives the expression of AC4 (AAV2/9-αMHC-AC4). The AAV viral particles were then administered intravenously via the tail vein and the mice were euthanized at 7 weeks after gene delivery. Our results showed that cardiac-specific *AC4* gene expression protected against Klotho deficiency-induced heart dysfunction and cardiac remodeling. AAV2/9-αMHC-AC4 increased cardiomyocytic cAMP levels, which alleviated PKA-dependent mitochondrial dysfunction, superoxide accumulation and apoptotic cell death. Our findings suggest that AC4 could be a potential therapeutic target for cardiomyopathy associated with Klotho deficiency in aging or chronic kidney disease.

Materials and Methods

The data, methods, and study materials are available on request by contacting the corresponding authors.

Animal Study Protocols

Klotho-hypomorphic mutant (KL (−/−)) mice were kindly provided by Dr. Kuro-o and were backcrossed to 129/SvJ mice for more than nine generations to achieve congenic background [13]. All KL (−/−) mice were fed with low phosphate diets containing with 0.2% inorganic phosphate (TD-09073, Harlan Teklad, Madison, WI) from weaning at 3 weeks of age. Low phosphate diets (0.2%) maintain serum phosphate in the normal range [17, 33]. Otherwise, KL (−/−) mice would die at 8–10 weeks old due to hyperphosphatemia. Normal phosphate diets contain 0.35% inorganic phosphate. AAV2/9-αMHC-AC4 (5×10^6 EP/ml, 150μl/mouse) was administered intravenously via the tail vein. Heart function was measured by cardiac magnetic resonance imaging (MRI) before sacrifice. Mice were euthanized at 7 weeks after gene delivery, and tissues were collected for correlative research. All animal experiment of this study was performed according to the guidelines of the National Institute of Health on the care and use of laboratory animals and approved by the Institutional Animal Care and Use Committee of University of Oklahoma Health Science Center.

AAV Vector Construction and Production

The procedures for plasmid construction and adeno-associated virus (AAV) packaging were described in our previous studies [17, 34–37]. The α-MHC promoter was used to direct cardiac specific AC4 expression. The truncated α-MHC promoter (160bp) and AC cDNA were then cloned into the AAV2 vector (Stratagene, La Jolla, CA) by replacing the CMV promoter (AAV-αMHC-AC4). GFP cDNA was cloned into the AAV2 vector with the same strategy as the control vector (AAV2-αMHC-GFP). The constructs of AAV2-αMHC-AC4 and AAV2-αMHC-GFP were then packaged in AAV/293 cells with pHelper and pAAV9-RC to produce AAV2/9 recombinant virus according to the instruction manual of AAV

Helper-Free System (Startagen, La Jolla, CA). The AAV2/9 purification was performed with ultracentrifugation in density-gradient iodixanol solution (Sigma, D1556). The virus titer was titrated in AAV-HT1080 cells according to the instruction manual of AAV Helper-Free System (Startagen, La Jolla, CA).

Cardiac magnetic resonance imaging

MRI analysis of heart function was carried out in a blinded fashion, i.e., the experimenters do not have knowledge of group identity. Briefly, *In vivo* MRI cardiac images were performed on a 7 Tesla MRI scanner (Bruker BioSpin, Ettlingen, Germany). The total LV volume at end diastole and end systole was estimated by taking the sum of all cavity slice volumes assuming a uniform thickness of excitation across a chosen slice at the two trigger points. For assessment of LV systolic and diastolic dynamics, the cavity slice volume was measured in all acquired images and was plotted against the time from onset of the QRS trigger, and a volume-time curve was established.

RNA sequencing analysis

Total RNAs from cardiomyocytes isolated from fresh ventricular tissue were isolated using Direct-zol™ RNA MiniPrep kit (Zymo Research, Irvine CA) and RNA qualities for each sample were analyzed using the Bioanalyzer 2100 and RNA 6000 nano kits (Agilent, Santa Clara CA). An RNA integrity number (RIN) of >6 is considered as a good RNA preparation. The cDNA library was constructed from 1.0 μg of total RNA using the TruSeq RNA library prep V2 kit (Illumina, San Diego, CA) and established protocols. Three samples per run were used for collecting sufficient data to determine the most highly expressed genes from each sample. A minimum of 30 million 250 bp paired end sequencing reads were collected on each run and data were analyzed using Genesifter software (Perkin Elmer, Boston, MA). Raw data for each sample were mapped to the most recent mouse genome build for identification of both exon and intergenic regions. Tertiary bioinformatics analysis (pairwise comparison) of the expression results were performed and information from both KEGGs and Gene Ontology databases were analyzed for identification of mRNAs that are differentially expressed at a significant level.

Cardiomyocytes size measurement

To quantify cardiomyocyte size, paraffin-embedded heart sections were stained with FITC–wheat germ agglutinin (SIGMA-ALDRICH) to delineate the cell membrane. The images were captured with fluorescence microscope (Olympus model 1X73) and analyzed by ImageJ software. Cardiomyocyte cross-sectional areas were measured from 400–500 cells per heart, 4 hearts per group.

Cardiac fibrosis and calcium deposition measurement

Hearts were perfused and excised from isoflurane-euthanized mice, washed in cold PBS. The upper and middle part of the hearts were fixed in 4% paraformaldehyde, embedded in paraffin and sectioned at 5 μm thickness. Collagen was quantified by masson's trichrome staining as we described previously [38]. The blue staining represented collagen deposition. A series of 4 sections of each mouse (4 mice per group) was examined and

photographed using an Olympus BH-L microscope coupled with a digital color camera. Using ImageJ software, blue-stained areas and non-stained myocyte areas from each section were determined using color-based thresholding. The percentage of total fibrosis area was calculated as the summed blue stained areas divided by total ventricular areas.

Cardiac calcium deposition was analyzed by using alizarin red staining kit (IHC WORLD, Woodstock, MD) as per the manufacturer's protocol. Calcification area was quantified with Image J as described above.

Cardiomyocyte isolation

Cardiomyocytes and fibroblasts were isolated by cardiomyocytes isolation kit (Cellutron Life Technology, Baltimore MD) as per the manufacturer's protocol. Briefly, mouse heart was dissected and digested with specific enzymatic medium. The digested cells were pre-plated for 1–2 hours to collect the cardiac fibroblasts as described previously. The unattached cells were then transferred into a new tube and spined at 1100 rpm for 2 min to collect the cardiomyocytes.

Western Blot Analysis

Western blot analysis was performed as we described previously [39–42]. Protein samples of the cardiomyocytes and fibroblasts isolated from the mouse hearts were prepared in RIPA lysis buffer. 30μg of total proteins were resolved by SDS-PAGE and transferred to a nitrocellulose membrane (Bio-Rad). Then the membranes were incubated overnight (4°C) with a primary antibody against AC4 (Sigma, SAB4300752, 1:1000), PKA (Cell Signaling, #5842, 1:1000), P-PKA (Cell Signaling, #5661, 1:1000), PLN (Cell Signaling, #14562, 1:1000), P-PLN (Cell Signaling, #8496, 1:1000), SERCA2 (Cell Signaling, #9580, 1:1000), Cleaved-caspase 3 (Cell Signaling, #9661, 1:1000), Epac1 (Abcam, ab109415, 1:1000), GAPDH (Santa Cruz, sc-32233, 1:1000). Goat anti-mouse or goat anti-rabbit horseradish peroxidase (1:2000–1:5,000; Santa Cruz Biotechnology) was used as a secondary antibody and incubated for 1 hour at room temperature. Specific proteins were detected by chemiluminescent methods using Clarity™ western ECL substrate (Bio-Rad, Hercules, CA). Protein abundance on western blots was quantified by densitometry using Image lab software (Bio-Rad, Hercules, CA).

Real-time PCR

Real-time RT-PCR was performed as we described previously [18, 43]. Total RNA was extracted using a Direct-zol ™ RNA Miniprep kit (Zymo Research, Irvine, CA) from the heart. Real-time RT-PCR was done using the TaqMan® Universal PCR Master Mix (Thermo Fisher, Foster city, CA) in a Bio-Rad C1000™ real-time PCR machine. The following gene-specific primers was used for amplifying AC4: forward, 5'-CCTCCTGGAGCCTAGCTTTG-3', reverse, 5'-GAGATCTTCGCTGGGAGGAG-3'. Reverse transcription was done using the iScript cDNA synthesis kit (Bio-Rad, Hercules, CA). The PCR condition was as follows: hold for 5 min at 94 °C, followed by 30 cycles consisting of denaturation at 94 °C (30 s), annealing at 57 °C (30 s), and elongation at 72 °C (1 min). After amplification protocol was over, PCR product was subjected to melt curve analysis using Bio-Rad CFX manager software. Fold change was calculated using the ΔΔ

threshold cycle method and the value for the GAPDH gene, which was normalized to WT groups.

Oxidative stress assay

The superoxide production was assessed by dihydroethidium (DHE) staining (Thermo Fisher Scientific Inc) as we described earlier [44, 45]. After deparaffinization and rehydration, the paraffin-embedded sections were then incubated with DHE (10^{-5} M) solution for 30 min at 37°C in the dark. Red fluorescence was examined and photographed with a fluorescence microscope (Olympus 1X73) in five randomly chosen fields from four independent experiments. Oxidative stress was expressed as gray volume of the DHE staining and analyzed using Image J (NIH).

Apoptosis assays

Apoptotic cells were detected by terminal deoxynucleotidyl transferase-mediated nick-end labeling (TUNEL) using the Click-iT® Plus TUNEL Assay Kit (Thermo Fisher, c10618) as per the manufacturer's protocol. TUNEL positive cells were expressed as a percentage of the total number of cells and analyzed using Image J (NIH). At least 200 cells were scored in each of four independent experiments.

Apoptosis was also evaluated by western blot analysis of cleaved caspase-3 expression.

ATP assay

The ATP level in the cardiomyocytes was measured using ATP assay kit (Abcam, ab83355, San Francisco, CA) following the manufacturer's instructions. The absorbance was read using the BioTek Synergy2 multi-mode microplate reader (BioTek Instruments, Winooski, VT).

cAMP assay

cAMP was measured using the Cyclic AMP XP chemiluminescent assay kit (Cell Signaling, 8019, Danvers, MA) following the manufacturer's instructions. Signals were measured using the BioTek Synergy2 multi-mode microplate reader (BioTek Instruments, Winooski, VT).

Mitochondrial complex I enzyme activity assay

Cardiac mitochondrion was isolated by using the mitochondria isolation kit (Abcam, San Francisco, CA). Mitochondrial enzyme activity was detected by the complex I enzyme activity microplate assay kit (Abcam, San Francisco, CA).

Statistical Analysis

Quantitative data were presented as the Means ± SEM. Differences between experimental groups were examined by unpaired t-test, or two-way ANOVA using Prism software (GraphPad). For all analysis, $p<0.05$ was considered statistically significant.

Results

The data that support the findings of this study are available from the corresponding author upon reasonable request.

Klotho deficiency-induced cardiac remodeling and dysfunction is associated with a decrease of AC4 expression

Left ventricular myocardial mass was significantly increased in 10-month-old KL (−/−) mice compared with age matched WT mice (Fig. 1A). Left ventricular wall thickness was also significantly increased in KL (−/−) mice (Fig. 1B). These data suggest that Klotho deficiency causes cardiac hypertrophy. Concomitantly, heart function declined significantly in KL (−/−) mice, as shown by decreases in the left ventricular end-diastolic volume, fractional shorting, ejection fraction, stroke volume and cardiac output (Fig. 1C–G). These results suggest that Klotho deficiency impairs cardiac function leading to heart failure.

We then performed RNA sequencing (RNA-seq) to profile the transcriptomes in isolated cardiomyocytes of KL (−/−) and WT mice. We identified a set of 304 genes that were differentially expressed in KL (−/−) mouse hearts: 227 genes were found to be upregulated and 77 genes were downregulated. Using the molecular pathways annotated in the Kyoto Encyclopedia of Genes and Genomes (KEGG), we found that the molecular pathway related to ‘dilated cardiomyopathy’ was dysregulated (Fig. 2A). In particular, the *AC4* gene expression level was decreased (Fig. 2A) while AC5 or AC6 gene expression levels were not altered (not shown) in cardiomyocytes in KL (−/−) mice. We next verified the altered expression of AC4 using quantitative RT-PCR (qRT-PCR) and WB in hearts from 10-month-old mice. Both the mRNA and protein expression of AC4 were significantly decreased by approximately 50% in KL (−/−) mice (Fig. 2B and C), which led us to explore whether AC4 may take part in Klotho deficiency-induced heart failure.

AAV-αMHC-AC4 protected against Klotho deficiency-induced cardiac dysfunction and remodeling

Therefore, AAV2/9-αMHC-AC4 was administered *via* tail vein to explore the effects of cardiac-specific *AC4* gene expression on Klotho deficiency-induced heart failure. The AAV.GFP transduction efficiency is 86.2 % in cardiomyocytes (Supplementary Fig. S1), indicating effective transduction. Although GFP-positive staining was found in the heart, it was not detectable in skeletal muscle or kidneys (Supplementary Fig. S4). The data confirm that AAV-AC4 expression is cardiac-specific. Intriguingly, seven weeks treatment of AAV2/9-αMHC-AC4 increased left ventricular fractional shorting, ejection fraction, stroke volume and end-diastolic volume in KL (−/−) mice (Fig. 3), suggesting that cardiac-specific AC4 gene expression prevents cardiac dysfunction in KL (−/−) mice.

Consistent with these results of cardiac function, AAV2/9-αMHC-AC4 also decreased heart weight to body weight ratio, left ventricular myocardial mass to body weight ratio, and left ventricular wall thickness in KL (−/−) mice (Fig. 4A, B and C). Cardiomyocyte cross-sectional areas were also significantly decreased by AAV2/9-αMHC-AC4 in KL (−/−) mice

(Fig. 4D). These results suggest that cardiac-specific *AC4* gene expression protects against Klotho deficiency-induced cardiac hypertrophy and remodeling.

AAV2/9-αMHC-AC4 did not affect body weight or kidney weight significantly in either WT or KL (−/−) mice (Supplementary Fig. S2, S3), indicating that AAV2/9-αMHC-AC4 did not have obvious toxic effects.

AAV-αMHC-AC4 alleviated Klotho deficiency-induced cardiac fibrosis and calcification

Heart remodeling are always followed by myocardial degeneration with extensive fibrosis and dystrophic calcification. Trichrome staining showed that cardiac-specific *AC4* gene expression decreased collagen deposition in the heart of KL (−/−) mice (Fig. 5A and C).

Alizarin red staining showed that cardiac-specific *AC4* gene delivery decreased calcium deposition in the heart of KL (−/−) mice (Fig. 5B and D).

AAV-αMHC-AC4 attenuated Klotho deficiency-induced increases in cardiac superoxide levels and cardiac apoptosis

Excessive superoxide causes myocardial damages which eventually leads to cell necrosis and/or apoptosis. We measured cardiac superoxide levels using DHE fluorescence staining and apoptosis using TUNEL labeling and western blot analysis of cleaved-caspase 3. As shown in Figure 6A, and C, the levels of DHE was significantly increased in the heart of KL (−/−) mice, indicating that Klotho deficiency increases superoxide accumulation. Cardiac-specific *AC4* gene expression decreased Klotho deficiency-induced superoxide accumulation (Fig. 6A, C).

Increased superoxide or reactive oxygen species could cause cell apoptosis [20, 46]. AAV-αMHC-AC4 attenuated the increases in TUNEL-positive cells and cleaved-caspase3 expression in the isolated cardiomyocytes of KL (−/−) mice (Fig. 6B, D, and E), suggesting that cardiac-specific *AC4* gene expression attenuated Klotho deficiency-induced cardiac apoptosis. Dual staining of TUNEL and cTnT indicated that the TUNEL positive cells are cardiomyocytes (Fig. 6B). Overall, Cardiac-specific *AC4* gene delivery rescued Klotho deficiency-induced increases in cardiac superoxide levels and apoptotic cell death.

AAV-αMHC-AC4 abolished Klotho deficiency-induced myocytes mitochondrial dysfunction via cAMP/PKA/PLN pathway

Cardiac ATP content was significantly decreased in in KL (−/−) mice, and AAV2/9-αMHC-AC4 rescued the ATP depletion (Fig. 7A). The activities of complex I was reduced in mitochondria isolated from KL (−/−) mouse hearts which was abolished by AAV2/9-αMHC-AC4 (Fig. 7B). These results suggest that cardiac-specific expression of *AC4* prevents against Klotho deficiency-induced cardiac mitochondrial dysfunction.

AAV2/9-αMHC-AC4 increased cardiomyocyte AC4 protein expression in both WT and KL (−/−) mice (Fig. 7C). The cAMP levels in cardiomyocytes were decreased in KL (−/−) mice which was rescued by AAV2/9-αMHC-AC4 (Fig. 7D). Cardiac-specific AC4 expression also increased PKA expression and activity in KL (−/−) mice (Fig. 7E–I). Concomitantly, cardiac-specific *AC4* gene expression increased the expression of Phospho-

PLN but decreased the SERCA2 expression (Fig. 7H, I). These results suggest that AAV2/9-αMHC-AC4 rescued Klotho deficiency-induced mitochondrial dysfunction through the cAMP/PKA/PLN signaling pathway in cardiomyocytes.

Discussion

Klotho deficiency causes cardiac dysfunction and remodeling in Klotho-hypomorphic mutant (KL (−/−)) mice (Fig. 1) [32, 47, 48]. Thus, Klotho is important in the maintenance of normal heart function. Klotho levels are decreased in patients with cardiovascular disease [26, 27]. The circulating Klotho level may represent a prognostic tool and therapeutic target for cardiovascular disease. *Klotho* gene is primarily expressed in the kidney tubule epithelial cells [24]. Our recent studies showed that serum level of Kotho protein is decreased tremendously in KL (−/−) mice [17, 28]. Kidney-specific knockout of *klotho* gene also significantly diminished serum level of Klotho [28, 33], indicating that the kidney is an important source of the circulating Klotho. Interestingly, *klotho* gene is not expressed in cardiomyocytes in mice [17, 28] although it was reported that Klotho may be expressed in human hearts [49]. Exogenous Klotho protein protects against aging or chronic kidney disease-induced cardiomyopathy [17, 50, 51]. Therefore, the circulating Klotho is important in the regulation of cardiac function [17]. Klotho is associated with cardiovascular morbidity and mortality in dialysis patients [52].

Klotho deficiency-induced cardiac remodeling and dysfunction is accompanied by a decrease of AC4 expression in the heart (Fig. 2). Interestingly, our results demonstrated that cardiac-specific *AC4* gene expression protected against Klotho deficiency-induced heart dysfunction and cardiac remodeling (Figs. 3–5). The AC family is composed of nine membrane-bound isoforms (AC 1–9) and one soluble isoform (sAC). Multiple distinct AC complexes exist in the heart and are important regulators of cardiac physiology. While great effort has been made to understand the composition and roles of these complexes, there are still many questions to be answered. Whether AC4 regulates cardiac function is largely unknown. Our findings suggest that downregulation of AC4 may mediate cardiac dysfunction and remodeling in KL (−/−) mice. AC4 could be a potential therapeutic target for heart failure associated with Klotho deficiency (e.g., aging, chronic kidney disease).

The specific mechanism by which AC4 improves cardiac remodeling and function in Klotho-deficient mice is likely *via* activation of cAMP pathway. cAMP is a major second messenger in many organs, particularly in the heart, where it regulates diverse physiological processes such as Ca^{2+} homeostasis, beating frequency and myocardial contractility as well as cell death [2]. In this study, we found that cAMP level in cardiomyocytes is significantly decreased in KL (−/−) mice which can be rescued by cardiac-specific *AC4* gene expression (Fig 7D). It is known that cAMP activates protein kinase A (PKA) to mediate diverse biological effects, including cardiac remodeling and dysfunction [2, 53]. In cardiomyocytes, cardiac-specific *AC4* gene expression increased PKA expression and activity (Fig 7E–I). Cardiac-specific *AC4* gene delivery increased the expression of Phospho-PLN, so decreased the SERCA2 expression (Fig 7H, I), which are critical in modulating calcium flux, mitochondrial function and cardiac apoptosis in KL (−/−) mice. Indeed, cardiac-specific *AC4* gene expression rescued Klotho deficiency-

induced mitochondrial dysfunction (Fig 7A, B), cardiac superoxide accumulation, and cardiomyocyte apoptosis (Fig 6). Taken together, AC4 increases cAMP levels which protects against cAMP-dependent mitochondrial dysfunction, superoxide accumulation and apoptotic cell death. Mitochondrial dysfunction leads to overproduction of superoxide which is linked to cell apoptosis and fibrosis formation [17, 48, 54]. Therefore, we believe that rescue of cardiomyocyte mitochondrial dysfunction and excessive superoxide generation contribute to the cardioprotective effect of *in vivo AC4* expression in Klotho-deficient mice.

Cardiac-directed expression of some isoforms of ACs (e.g., AC8) may lead to an obvious compartmentation of the cAMP levels [55]. A limitation of this study is that we did not assess the sub-compartments of AC activity. In this experiment, we used AAV2/9-αMHC-GFP and PBS as control treatments. The ideal control for these experiments would be *in vivo* expression of an enzymatically inactive form of AC4, which is the limitation of this study.

The sarcoendoplasmic reticulum (SR) calcium transport ATPase (SERCA) is a pump that transports calcium ions from the cytoplasm into the SR. The SERCA pump is encoded by a family of three genes, SERCA1, 2, and 3, that are highly conserved but localized on different chromosomes. SERCA2 is the major isoform of *SERCA* expressed in cardiomyocytes. SERCA2 expression and activity are decreased in some pathophysiological conditions including heart failure [56]. The decreased SERCA2 activity causes hypocalcemia, which leads to heart failure. However, SERCA2 is increased in KL (−/−) mice (Fig. 7), suggesting that Klotho deficiency upregulates SERCA2 activity. Although the mechanism of Klotho deficiency-induced upregulation of SERCA2 remains to be found, overactive SERCA2 may cause calcium deposition in the myocardium leading to calcification (Figure 5B,D). Calcification also impairs heart function which contributes to heart failure. Thus, abnormal upregulation or downregulation of SERCA2 can impair heart function.

In the KL (−/−) model, expression AC4 (but not AC5/6) were decreased which plays an important role in the pathogenesis of heart failure. Cardiac-specific expression of AC4 effectively rescued Klotho deficiency-induced heart failure (Fig. 3). Viral delivery of AC6 showed promising cardiac protective effects in other models of heart failure [7, 57]. A randomized clinical trial demonstrated that viral-based *AC6* gene transfer increased LV function in patient with heart failure [58]. In a different model, however, *AC5* gene knockout prevents cardiomyopathy due to enhanced β-adrenergic signaling [59]. Similarly, cardiac-directed *AC6* gene mutation attenuates the deleterious effects of continuous β-adrenergic stimulation [60]. Therefore, the effect of AC on heart failure depends on models. Sustained stimulation of β1-adrenergic receptors increases the intracellular cAMP levels. In this case, inhibition or disruption of AC may be effective in improving heart failure.

In summary, we demonstrate in the Klotho deficiency-induced heart failure model that cardiac-specific *AC4* gene expression can markedly improve left ventricular function and structure. The beneficial effects are likely attributed to a rescue of downregulation of the cAMP-PKA pathway, mitochondrial dysfunction and apoptotic cell death in KL (−/−) mice (Supplementary Fig. S5). Further studies are warranted to investigate whether AC4 can serve

as a therapeutic target for heart failure associated with Klotho deficiency in aging or chronic kidney diseases (CKD).

Clinical Perspectives

Heart failure is the major cause of mortality in patients with chronic kidney disease (CKD). A decrease in Klotho levels is linked to CKD. Here we report that Klotho deficiency causes heart failure *via* downregulation of cardiac *AC4* gene expression. Importantly, cardiac-specific *AC4* gene expression markedly improves cardiac function and structure. These findings provide new therapeutic strategies for heart failure associated with CKD.

Translational Outlook

This study suggests that Klotho insufficiency may be involved in cardiomyopathy and heart failure associated with aging and CKD. We expect that treatment with Klotho or cardiac-specific expression of *AC4* gene would be effective in the control of heart failure in CKD patients. Human Klotho protein is immediately available for a clinical test in human heart failure. AAV is a safe vector and has been approved by FDA for clinical trial. AAV-αMHC-AC4 can be used for testing a novel cardiac-specific therapy for heart failure. Thus, the translation value of the finding is high.

Supplementary Material

Refer to Web version on PubMed Central for supplementary material.

Acknowledgment

This work was supported by NIH R01 AG062375, AG049780 and HL122166.

Data Availability

The data that support the findings of this study are available from the corresponding author upon reasonable request.

References

[1]. Virani SS, Alonso A, Aparicio HJ, Benjamin EJ, Bittencourt MS, Callaway CW, et al. Heart Disease and Stroke Statistics-2021 Update: A Report From the American Heart Association. Circulation. 2021;143:e254–e743. [PubMed: 33501848]

[2]. Wang Z, Liu D, Varin A, Nicolas V, Courilleau D, Mateo P, et al. A cardiac mitochondrial cAMP signaling pathway regulates calcium accumulation, permeability transition and cell death. Cell death & disease. 2016;7:e2198. [PubMed: 27100892]

[3]. Qasim H, McConnell BK. AKAP12 Signaling Complex: Impacts of Compartmentalizing cAMP-Dependent Signaling Pathways in the Heart and Various Signaling Systems. J Am Heart Assoc. 2020;9:e016615. [PubMed: 32573313]

[4]. Fenske S, Hennis K, Rötzer RD, Brox VF, Becirovic E, Scharr A, et al. cAMP-dependent regulation of HCN4 controls the tonic entrainment process in sinoatrial node pacemaker cells. Nature communications. 2020;11:5555.

[5]. Feldman AM. Adenylyl cyclase: a new target for heart failure therapeutics. Circulation. 2002;105:1876–8. [PubMed: 11997269]

[6]. Iwatsubo K, Bravo C, Uechi M, Baljinnyam E, Nakamura T, Umemura M, et al. Prevention of heart failure in mice by an antiviral agent that inhibits type 5 cardiac adenylyl cyclase. Am J Physiol Heart Circ Physiol. 2012;302:H2622–8. [PubMed: 22505646]

[7]. Lai NC, Tang T, Gao MH, Saito M, Takahashi T, Roth DM, et al. Activation of cardiac adenylyl cyclase expression increases function of the failing ischemic heart in mice. J Am Coll Cardiol. 2008;51:1490–7. [PubMed: 18402905]

[8]. Zhao Z, Babu GJ, Wen H, Fefelova N, Gordan R, Sui X, et al. Overexpression of adenylyl cyclase type 5 (AC5) confers a proarrhythmic substrate to the heart. American journal of physiology Heart and circulatory physiology. 2015;308:H240–9. [PubMed: 25485900]

[9]. Li Y, Hof T, Baldwin TA, Chen L, Kass RS, Dessauer CW. Regulation of I(Ks) Potassium Current by Isoproterenol in Adult Cardiomyocytes Requires Type 9 Adenylyl Cyclase. Cells. 2019;8.

[10]. Mewes M, Lenders M, Stappers F, Scharnetzki D, Nedele J, Fels J, et al. Soluble adenylyl cyclase (sAC) regulates calcium signaling in the vascular endothelium. FASEB journal : official publication of the Federation of American Societies for Experimental Biology. 2019;33:13762–74. [PubMed: 31585052]

[11]. Kleinboelting S, Diaz A, Moniot S, van den Heuvel J, Weyand M, Levin LR, et al. Crystal structures of human soluble adenylyl cyclase reveal mechanisms of catalysis and of its activation through bicarbonate. Proc Natl Acad Sci U S A. 2014;111:3727–32. [PubMed: 24567411]

[12]. Phan HM, Gao MH, Lai NC, Tang T, Hammond HK. New signaling pathways associated with increased cardiac adenylyl cyclase 6 expression: implications for possible congestive heart failure therapy. Trends Cardiovasc Med. 2007;17:215–21. [PubMed: 17936202]

[13]. Kuro-o M, Matsumura Y, Aizawa H, Kawaguchi H, Suga T, Utsugi T, et al. Mutation of the mouse klotho gene leads to a syndrome resembling ageing. Nature. 1997;390:45–51. [PubMed: 9363890]

[14]. Kurosu H, Yamamoto M, Clark JD, Pastor JV, Nandi A, Gurnani P, et al. Suppression of aging in mice by the hormone Klotho. Science. 2005;309:1829–33. [PubMed: 16123266]

[15]. Dubal DB, Yokoyama JS, Zhu L, Broestl L, Worden K, Wang D, et al. Life extension factor klotho enhances cognition. Cell reports. 2014;7:1065–76. [PubMed: 24813892]

[16]. Haruna Y, Kashihara N, Satoh M, Tomita N, Namikoshi T, Sasaki T, et al. Amelioration of progressive renal injury by genetic manipulation of Klotho gene. Proceedings of the National Academy of Sciences of the United States of America. 2007;104:2331–6. [PubMed: 17287345]

[17]. Chen K, Wang S, Sun QW, Zhang B, Ullah M, Sun Z. Klotho Deficiency Causes Heart Aging via Impairing the Nrf2-GR Pathway. Circ Res. 2021;128:492–507. [PubMed: 33334122]

[18]. Varshney R, Ali Q, Wu C, Sun Z. Monocrotaline-Induced Pulmonary Hypertension Involves Downregulation of Antiaging Protein Klotho and eNOS Activity. Hypertension. 2016;68:1255–63. [PubMed: 27672025]

[19]. Hu MC, Shi M, Zhang J, Quiñones H, Griffith C, Kuro-o M, et al. Klotho deficiency causes vascular calcification in chronic kidney disease. J Am Soc Nephrol. 2011;22:124–36. [PubMed: 21115613]

[20]. Lin Y, Sun Z. Antiaging Gene Klotho Attenuates Pancreatic beta-Cell Apoptosis in Type 1 Diabetes. Diabetes. 2015;64:4298–311. [PubMed: 26340932]

[21]. Lin Y, Sun Z. In vivo pancreatic beta-cell-specific expression of antiaging gene Klotho: a novel approach for preserving beta-cells in type 2 diabetes. Diabetes. 2015;64:1444–58. [PubMed: 25377875]

[22]. Mencke R, Hillebrands JL, consortium N. The role of the anti-ageing protein Klotho in vascular physiology and pathophysiology. Ageing research reviews. 2017;35:124–46. [PubMed: 27693241]

[23]. Wolf I, Levanon-Cohen S, Bose S, Ligumsky H, Sredni B, Kanety H, et al. Klotho: a tumor suppressor and a modulator of the IGF-1 and FGF pathways in human breast cancer. Oncogene. 2008;27:7094–105. [PubMed: 18762812]

[24]. Xu Y, Sun Z. Molecular basis of Klotho: from gene to function in aging. Endocr Rev. 2015;36:174–93. [PubMed: 25695404]

[25]. Wang Y, Sun Z. Current understanding of klotho. Ageing Res Rev. 2009;8:43–51. [PubMed: 19022406]

[26]. Seiler S, Rogacev KS, Roth HJ, Shafein P, Emrich I, Neuhaus S, et al. Associations of FGF-23 and sKlotho with cardiovascular outcomes among patients with CKD stages 2–4. Clinical journal of the American Society of Nephrology : CJASN. 2014;9:1049–58. [PubMed: 24677555]

[27]. Semba RD, Cappola AR, Sun K, Bandinelli S, Dalal M, Crasto C, et al. Plasma klotho and cardiovascular disease in adults. Journal of the American Geriatrics Society. 2011;59:1596–601. [PubMed: 21883107]

[28]. Chen K, Zhang B, Sun Z. MicroRNA 379 Regulates Klotho Deficiency-Induced Cardiomyocyte Apoptosis Via Repression of Smurf1. Hypertension. 2021;78:342–52. [PubMed: 34120450]

[29]. Lin Y, Sun Z. Klotho deficiency-induced arterial calcification involves osteoblastic transition of VSMCs and activation of BMP signaling. J Cell Physiol. 2021.

[30]. Kanbay M, Demiray A, Afsar B, Covic A, Tapoi L, Ureche C, et al. Role of Klotho in the Development of Essential Hypertension. Hypertension. 2021;77:740–50. [PubMed: 33423524]

[31]. Lv J, Chen J, Wang M, Yan F. Klotho alleviates indoxyl sulfate-induced heart failure and kidney damage by promoting M2 macrophage polarization. Aging (Albany NY). 2020;12:9139–50. [PubMed: 32464602]

[32]. Xie J, Cha SK, An SW, Kuro OM, Birnbaumer L, Huang CL. Cardioprotection by Klotho through downregulation of TRPC6 channels in the mouse heart. Nat Commun. 2012;3:1238. [PubMed: 23212367]

[33]. Wang Q, Wang S, Sun Z. Kidney-Specific Klotho Gene Deletion Causes Aortic Aneurysm via Hyperphosphatemia. Hypertension. 2021;78:308–19. [PubMed: 34176284]

[34]. Wang Y, Sun Z. Klotho gene delivery prevents the progression of spontaneous hypertension and renal damage. Hypertension. 2009;54:810–7. [PubMed: 19635988]

[35]. Gao D, Wang S, Lin Y, Sun Z. In vivo AAV delivery of glutathione reductase gene attenuates anti-aging gene klotho deficiency-induced kidney damage. Redox Biol. 2020;37:101692. [PubMed: 32863229]

[36]. Lin Y, Sun Z. Antiaging Gene Klotho Attenuates Pancreatic β-Cell Apoptosis in Type 1 Diabetes. Diabetes. 2015;64:4298–311. [PubMed: 26340932]

[37]. Lin Y, Sun Z. In vivo pancreatic β-cell-specific expression of antiaging gene Klotho: a novel approach for preserving β-cells in type 2 diabetes. Diabetes. 2015;64:1444–58. [PubMed: 25377875]

[38]. Chen J, Fan J, Wang S, Sun Z. Secreted Klotho Attenuates Inflammation-Associated Aortic Valve Fibrosis in Senescence-Accelerated Mice P1. Hypertension. 2018;71:877–85. [PubMed: 29581213]

[39]. Feng R, Ullah M, Chen K, Ali Q, Lin Y, Sun Z. Stem cell-derived extracellular vesicles mitigate ageing-associated arterial stiffness and hypertension. J Extracell Vesicles. 2020;9:1783869. [PubMed: 32939234]

[40]. Zhou X, Chen K, Lei H, Sun Z. Klotho gene deficiency causes salt-sensitive hypertension via monocyte chemotactic protein-1/CC chemokine receptor 2-mediated inflammation. J Am Soc Nephrol. 2015;26:121–32. [PubMed: 24904083]

[41]. Zhou X, Chen K, Wang Y, Schuman M, Lei H, Sun Z. Antiaging Gene Klotho Regulates Adrenal CYP11B2 Expression and Aldosterone Synthesis. J Am Soc Nephrol. 2016;27:1765–76. [PubMed: 26471128]

[42]. Chen J, Lin Y, Sun Z. Deficiency in the anti-aging gene Klotho promotes aortic valve fibrosis through AMPKα-mediated activation of RUNX2. Aging Cell. 2016;15:853–60. [PubMed: 27242197]

[43]. Han X, Sun Z. Epigenetic Regulation of KL (Klotho) via H3K27me3 (Histone 3 Lysine [K] 27 Trimethylation) in Renal Tubule Cells. Hypertension. 2020;75:1233–41. [PubMed: 32223380]

[44]. Ullah M, Sun Z. Klotho Deficiency Accelerates Stem Cells Aging by Impairing Telomerase Activity. J Gerontol A Biol Sci Med Sci. 2019;74:1396–407. [PubMed: 30452555]

[45]. Gao D, Zuo Z, Tian J, Ali Q, Lin Y, Lei H, et al. Activation of SIRT1 Attenuates Klotho Deficiency-Induced Arterial Stiffness and Hypertension by Enhancing AMP-Activated Protein Kinase Activity. Hypertension. 2016;68:1191–9. [PubMed: 27620389]

[46]. Shi L, Wu Y, Lv DL, Feng L. Scutellarein selectively targets multiple myeloma cells by increasing mitochondrial superoxide production and activating intrinsic apoptosis pathway. Biomed Pharmacother. 2019;109:2109–18. [PubMed: 30551468]

[47]. Hu MC, Shi M, Cho HJ, Adams-Huet B, Paek J, Hill K, et al. Klotho and phosphate are modulators of pathologic uremic cardiac remodeling. Journal of the American Society of Nephrology : JASN. 2015;26:1290–302. [PubMed: 25326585]

[48]. Chen K, Sun Z. Estrogen inhibits renal Na-Pi Co-transporters and improves klotho deficiency-induced acute heart failure. Redox Biol. 2021;47:102173. [PubMed: 34678656]

[49]. Liu Q, Zhu LJ, Waaga-Gasser AM, Ding Y, Cao M, Jadhav SJ, et al. The axis of local cardiac endogenous Klotho-TGF-β1-Wnt signaling mediates cardiac fibrosis in human. J Mol Cell Cardiol. 2019;136:113–24. [PubMed: 31520610]

[50]. Xie J, Yoon J, An SW, Kuro-o M, Huang CL. Soluble Klotho Protects against Uremic Cardiomyopathy Independently of Fibroblast Growth Factor 23 and Phosphate. Journal of the American Society of Nephrology : JASN. 2015;26:1150–60. [PubMed: 25475745]

[51]. Yang K, Wang C, Nie L, Zhao X, Gu J, Guan X, et al. Klotho Protects Against Indoxyl Sulphate-Induced Myocardial Hypertrophy. J Am Soc Nephrol. 2015;26:2434–46. [PubMed: 25804281]

[52]. Marcais C, Maucort-Boulch D, Drai J, Dantony E, Carlier MC, Blond E, et al. Circulating Klotho Associates With Cardiovascular Morbidity and Mortality During Hemodialysis. The Journal of clinical endocrinology and metabolism. 2017;102:3154–61. [PubMed: 28402487]

[53]. de Rooij J, Zwartkruis FJ, Verheijen MH, Cool RH, Nijman SM, Wittinghofer A, et al. Epac is a Rap1 guanine-nucleotide-exchange factor directly activated by cyclic AMP. Nature. 1998;396:474–7. [PubMed: 9853756]

[54]. Wang X, Wang Q, Sun Z. Normal IgG downregulates the intracellular superoxide level and attenuates migration and permeability in human aortic endothelial cells isolated from a hypertensive patient. Hypertension. 2012;60:818–26. [PubMed: 22777940]

[55]. Georget M, Mateo P, Vandecasteele G, Jurevicius J, Lipskaia L, Defer N, et al. Augmentation of cardiac contractility with no change in L-type Ca2+ current in transgenic mice with a cardiac-directed expression of the human adenylyl cyclase type 8 (AC8). FASEB J. 2002;16:1636–8. [PubMed: 12206999]

[56]. Park WJ, Oh JG. SERCA2a: a prime target for modulation of cardiac contractility during heart failure. BMB Rep. 2013;46:237–43. [PubMed: 23710633]

[57]. Lai NC, Roth DM, Gao MH, Tang T, Dalton N, Lai YY, et al. Intracoronary adenovirus encoding adenylyl cyclase VI increases left ventricular function in heart failure. Circulation. 2004;110:330–6. [PubMed: 15249510]

[58]. Hammond HK, Penny WF, Traverse JH, Henry TD, Watkins MW, Yancy CW, et al. Intracoronary Gene Transfer of Adenylyl Cyclase 6 in Patients With Heart Failure: A Randomized Clinical Trial. JAMA Cardiol. 2016;1:163–71. [PubMed: 27437887]

[59]. Yan L, Vatner SF, Vatner DE. Disruption of type 5 adenylyl cyclase prevents β-adrenergic receptor cardiomyopathy: a novel approach to β-adrenergic receptor blockade. Am J Physiol Heart Circ Physiol. 2014;307:H1521–8. [PubMed: 25193472]

[60]. Gao MH, Lai NC, Giamouridis D, Kim YC, Guo T, Hammond HK. Cardiac-directed expression of a catalytically inactive adenylyl cyclase 6 protects the heart from sustained β-adrenergic stimulation. PLoS One. 2017;12:e0181282. [PubMed: 28767701]

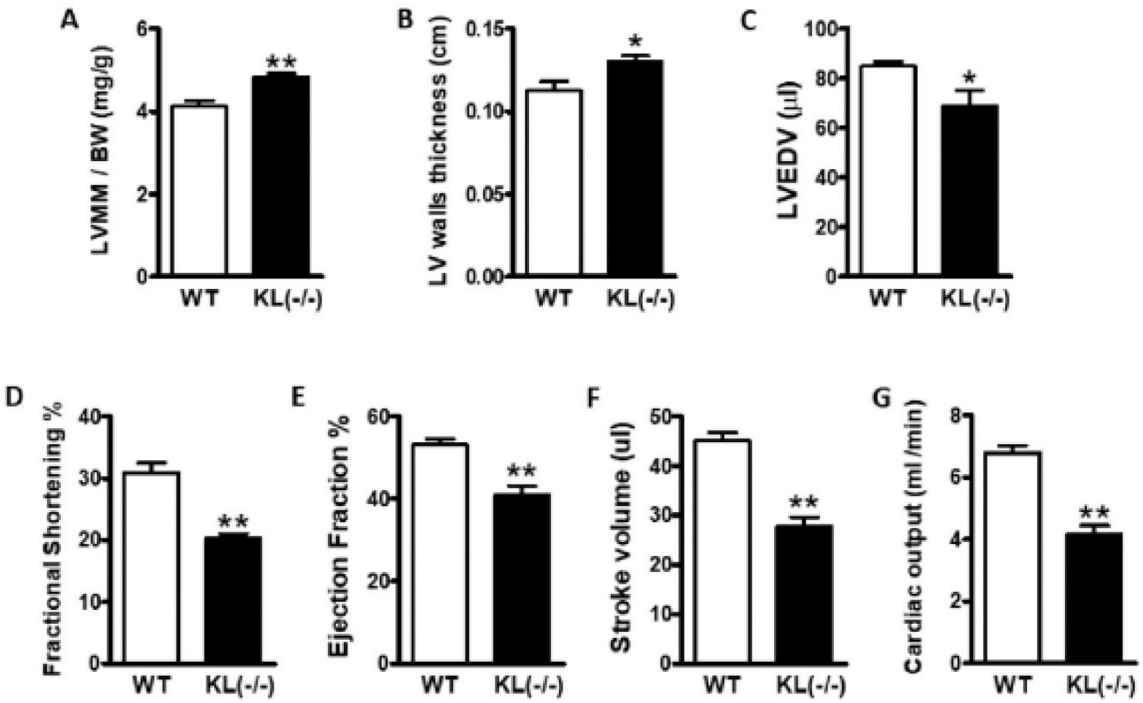

Fig 1. Klotho deficiency caused cardiac hypertrophy and dysfunction.

Cardiac function was measured by MRI in 10-month-old KL (−/−) male mice fed with low-phosphate diets and age-matched WT mice. (A) Left ventricular (LV) myocardial mass to body weight ratio. (B) LV walls thickness. (C) LV end-diastolic volume. (D) LV fractional shortening. (E) LV ejection fraction. (F) Stroke volume. (G) Cardiac output. Data are expressed as means ± SEM and analyzed by t-test, *p<0.05, **p<0.01 vs wild type mice, n=5.

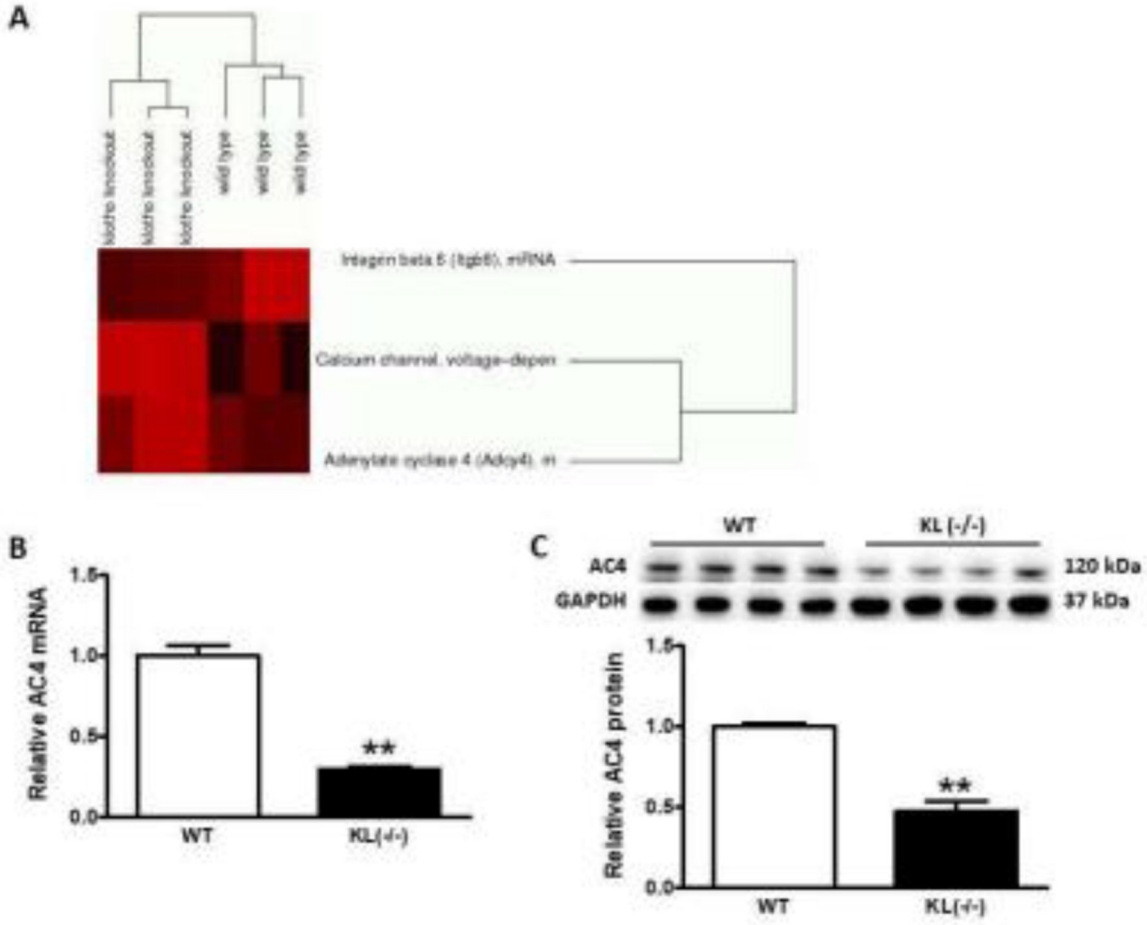

Fig 2. AC4 gene and protein expression was decreased in KL (−/−) mice.

(A) Dysregulated mRNA of the molecular pathway related to dilated cardiomyopathy measured by RNA sequencing analysis. (B) qRT-PCR analysis of AC4 mRNA expression. (C) Western blot analysis of AC4 protein expression. Data are expressed as means ± SEM and analyzed by t-test, **p<0.01 vs wild type mice, n=4.

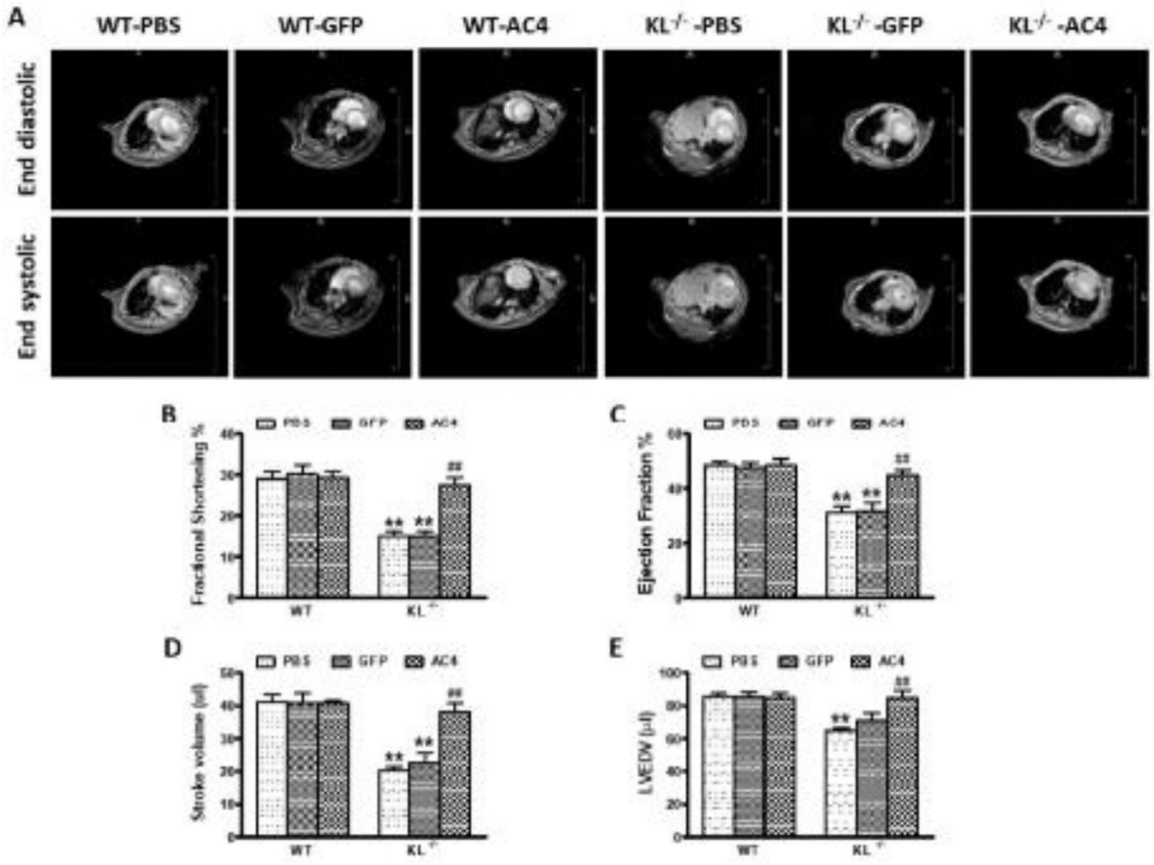

Fig 3. AAV-αMHC-AC4 protected against Klotho deficiency-induced heart dysfunction.

Cardiac function was measured by MRI. (A) Representative cardiac MRI images. (B) LV fractional shortening. (C) LV ejection fraction. (D) Stroke volume. (E) LV end-diastolic volume. Data are expressed as means ± SEM and analyzed by two-way ANOVA, **p<0.01 vs WT-PBS group, $^{\#\#}$p<0.01 vs KL (−/−)-PBS group, n=4–7.

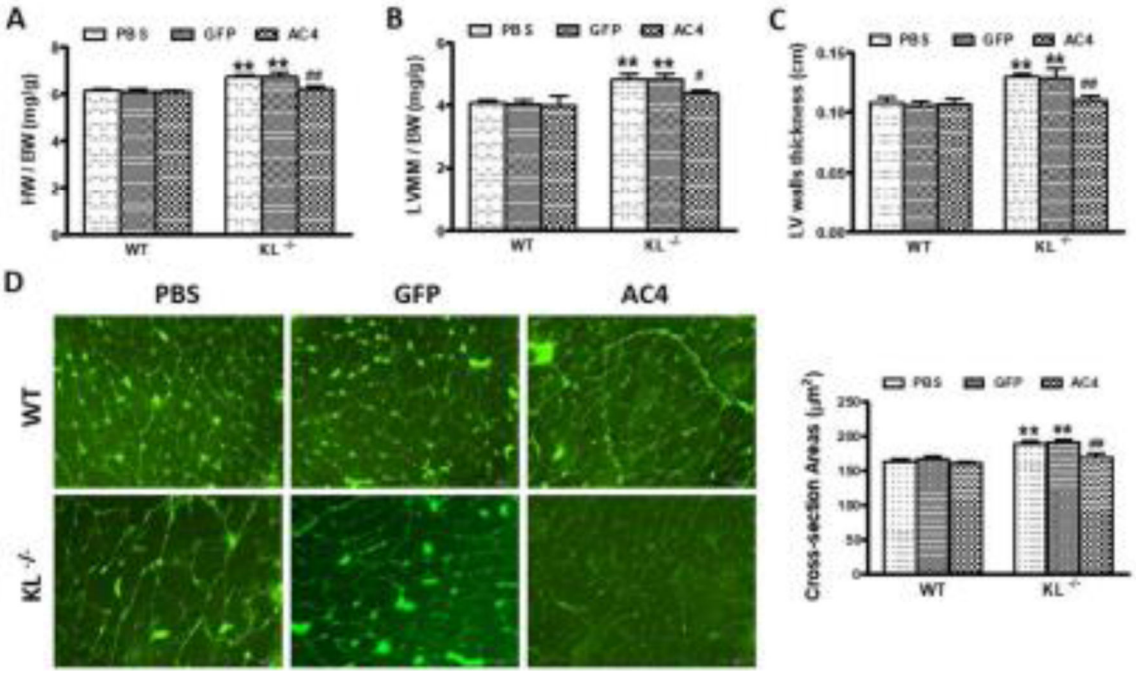

Fig 4. AAV-αMHC-AC4 protected against Klotho deficiency-induced cardiac hypertrophy.

(A) Heart weight to body weight ratio. n=4–7. (B) LV myocardial mass to body weight ratio. n=4–7. (C) LV walls thickness. n=4–7. (D) Cardiomyocyte cross-section area by WGA staining. n=4. Data are expressed as means ± SEM and analyzed by two-way ANOVA, **p<0.01 vs WT-PBS group, #p<0.05, ##p<0.01 vs KL (−/−)-PBS group.

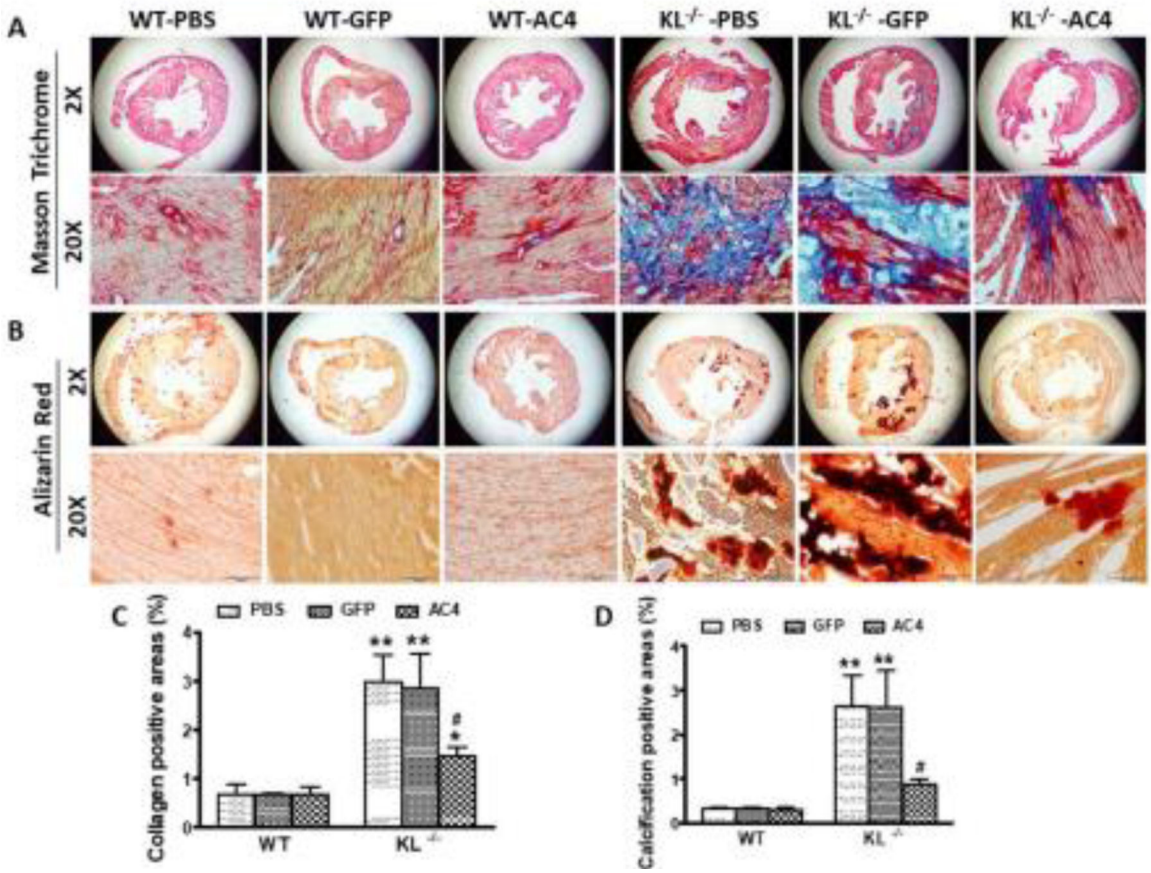

Fig 5. AAV-αMHC-AC4 alleviated Klotho deficiency-induced cardiac fibrosis and calcification.

(A) Representative images of masson's trichrome staining. (B) Representative images of alizarin red staining. (C) Quantification of fibrosis by trichrome staining. (D) Quantification of calcification by alizarin red staining. Data are expressed as means ± SEM and analyzed by two-way ANOVA, *p<0.05, **p<0.01 vs WT-PBS group, #p<0.05 vs KL (−/−)-PBS group, n=4.

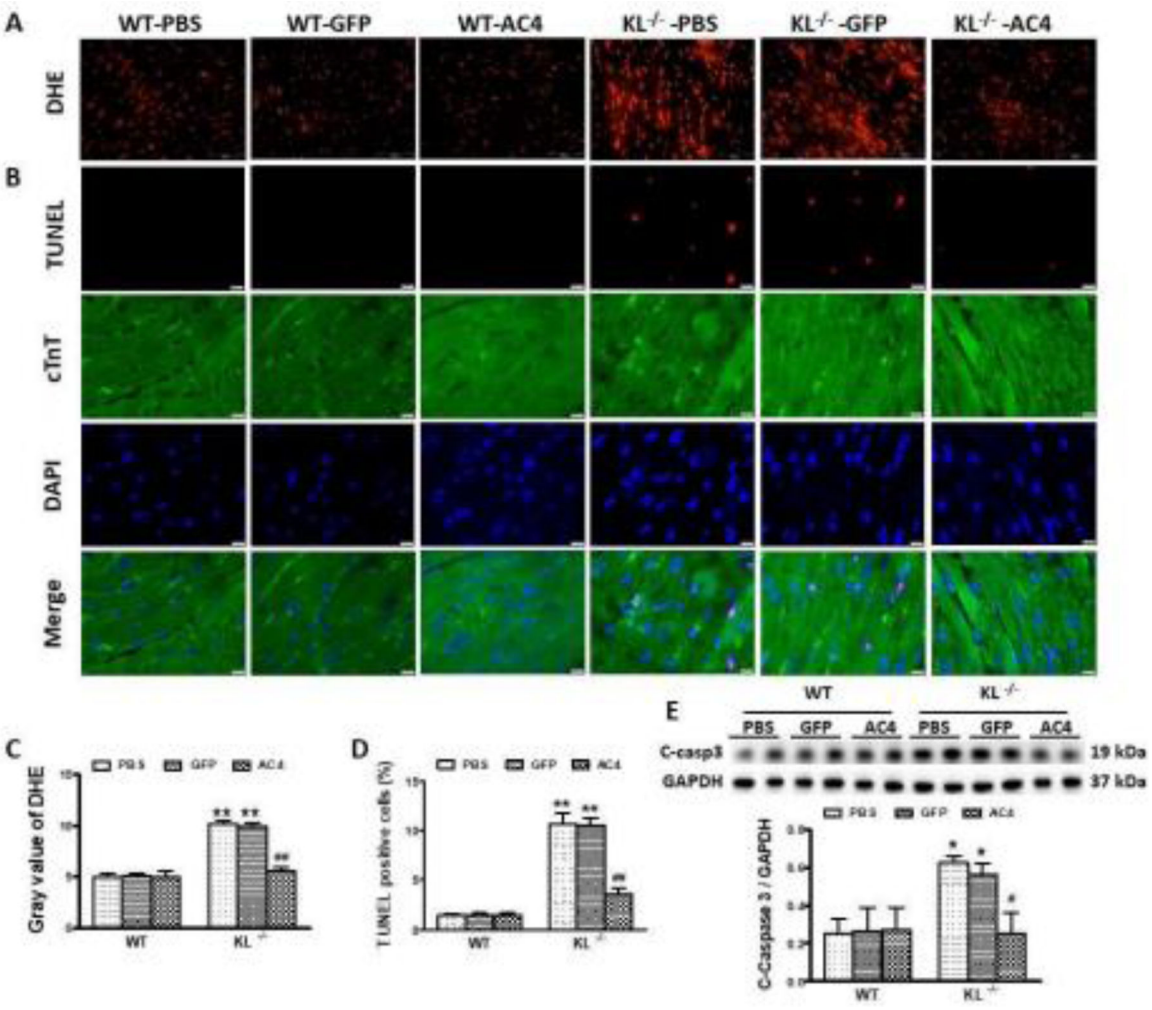

Fig 6. AAV-αMHC-AC4 attenuated Klotho deficiency-induced increases in superoxide levels and cardiac apoptosis.

(A) Representative images of DHE staining. (B) Dual staining of TUNEL (apoptosis marker) and cTnT (cardiomyocyte marker). (C) Quantification of superoxide levels by DHE staining. n=4. (D) Quantification of cardiac apoptosis by TUNEL labelling. (E) Western blot analysis of cleaved caspase 3 (C-caspase 3). Data are expressed as means ± SEM and analyzed by two-way ANOVA, *p<0.05, **p<0.01 vs WT-PBS group, #p<0.05, ##p<0.01 vs KL (−/−)-PBS group, n=4.

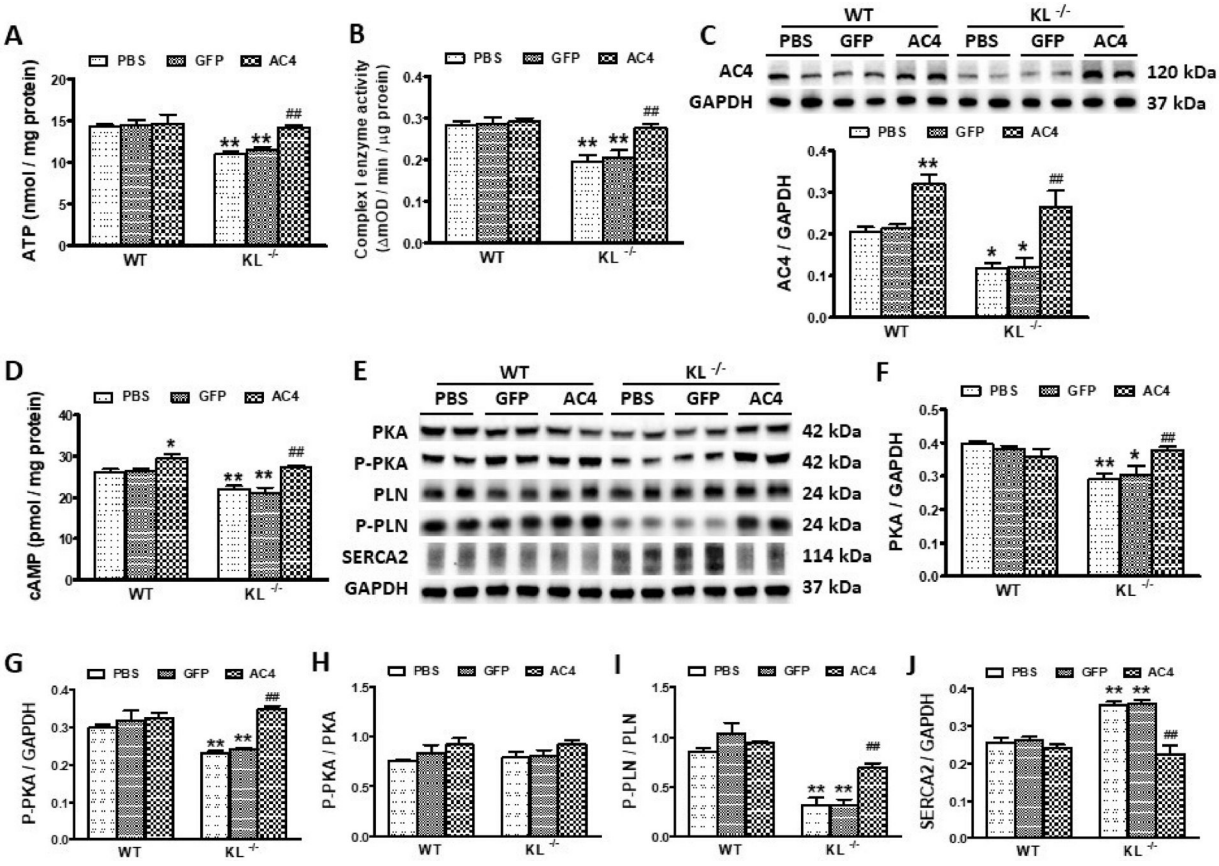

Fig 7. AAV-αMHC-AC4 abolished Klotho deficiency-induced cardiomyocyte mitochondrial dysfunction.

Cardiomyocytes were isolated from the mice heart by cardiomyocytes isolation kit. (A) Cardiomyocyte ATP content. (B) Mitochondrial complex I enzyme activity. (C) Western blot analysis of AC4 in cardiomyocytes. (D) Cardiomyocyte cAMP generation. (E) Western blot analysis of PKA, Phospho-PKA, PLN, Phospho-PLN, SERCA2. (F) Quantification of PKA expression. (G) Quantification of Phospho-PKA expression. (H) Quantification of Phospho-PKA to total PKA. (I) Quantification of Phospho-PLN expression. (J) Quantification of SERCA2 expression. Data are expressed as means ± SEM and analyzed by two-way ANOVA, *p<0.05, **p<0.01 vs WT-PBS group, ##p<0.01 vs KL (−/−)-PBS group, n=4.